

Thermal efficiency improvement of a solar desalination process by parabolic trough collector

Randha Bellatreche, Maamar Ouali, Mourad Balistrrou and Djilali Tassalit

ABSTRACT

Nexus water/energy security is one of the main global challenges for the future generation. Solar distillation (thermal process) represents a sustainable solution to water shortages and energy crisis in the world especially in the Middle East and North Africa region. The technique is based on a evaporation–condensation process via heat delivery through a cylindrical parabolic collector to a thermal energy storage, in the form of sand integrated into the solar still, to maximize water production efficiencies. It is a technically feasible and operational method. Results suggest that the additional solar collector flux has a direct impact on the increase in average sand and seawater temperature particularly over the period between 12 p.m. and 4 p.m. Seawater temperature increases by >26.6%. The energy stored quantity delivered for the distiller basin grows proportionality with the sand temperature, which is depending directly for the solar collector absorber temperature. The difference between the both temperatures defines a decreasing rate of –19%. The daily water production by the hybrid solar distiller is 6.5 l/day, it represents an increase of +91% compared to the traditional concrete solar still production (3.4 l/day), for the same geometry and meteorological conditions.

Key words | cylindrical parabolic collector, parabolic trough collector, solar distillation, solar still, thermal energy storage

HIGHLIGHTS

- Renewable energies integration in the seawater distillation process.
- Improvement of the water evaporation phenomenon using a parabolic trough solar concentrator.
- Solar still efficiency optimization by the thermal energy storage integration.
- New design of the greenhouse still flow control principle, materials.
- Proved the efficiency of the hybrid still compared to the concrete still in a Mediterranean climate.

This is an Open Access article distributed under the terms of the Creative Commons Attribution Licence (CC BY-NC-ND 4.0), which permits copying and redistribution for non-commercial purposes with no derivatives, provided the original work is properly cited (<http://creativecommons.org/licenses/by-nc-nd/4.0/>)

doi: 10.2166/ws.2021.131

Randha Bellatreche (corresponding author)
Department of Renewable Energy,
Technology Faculty,
University Saad Dahlab Blida1,
BP270 Soumaa Road, Blida 09000,
Algeria
E-mail: bellatreche_randa@yahoo.fr

Maamar Ouali
Djilali Tassalit
Unité de Développement des Equipements
Solaires,
UDES/Centre de Développement des Energies
Renouvelables, CDER,
Bou-Ismaïl, 42415, Tipaza,
Algérie

Mourad Balistrrou
Mechanical Engineering Department,
Engineering Science Faculty,
University M'hamed Bougara,
Independence Avenue, 35000, Boumerdes,
Algeria

NOMENCLATURE

ABBREVIATIONS

MENA	Middle East and North Africa
UDES	Unité de Développements des Equipements Solaire
WHO	World Health Organization
UNICEF	United Nations International Children's Emergency Fund
ENR	Renewable Energies
CFD	Computational Fluid Dynamic
CSP	Concentrated Solar Power
CPC	Cylindrical Parabolic Collector
TES	Thermal Energy Storage

e	Evaporation
r	Radiation
f	Heat transfer fluid
D	Distiller basin
S	Sand
0	Initial
abs	Absorber
exch	Exchanger
ref	Reflector
max	Maximum
avg	Average

SYMBOLS

A	Area (m^2)
e	Thickness (m)
M	Mass (kg)
V	Velocity (m/s)
V _f	Heat transfer fluid velocity (m/s)
Re	Reynolds number
T	Temperature (K)
K	Thermal conductivity (W/m.K)
L	Latent heat of water vaporization (J/kg)
C _p	Specific heat [C _w] (J/kg.K)
h	Heat transfer coefficient (W/m ² .K)
Q	Heat flux (W/m ²)
\dot{Q}	Total heat transfer rate
I	Incident solar intensity (W/m ²)
α'	Fraction of solar flux absorbed
ϵ	Emissivity
P	Partial saturated vapor pressure (N/m ²)
Pr	Hourly yield (l)
t	Time (s)
C _f	Geometric concentration factor

SUBSCRIPTS

a	Ambient
g	Glance
i	Inner
o	Outer
w	Water
c	Convection

INTRODUCTION

Nexus water/energy security is one of the main global challenges in impact terms on the next future generation. Today, 70% of water is used for agriculture. To feed 9.7 billion people by 2050, agricultural production and water share must increase by 60% and 15%, respectively (Eau 2019). A significant decrease in quality and quantity of available freshwater has harmful effects on human health and economic activity (The Global Risks Report 2016). According to a report published by WHO and UNICEF (UNICEF 2017), three out of ten people (3/10) worldwide do not have access to safe and easily accessible water in their homes; while the Kyoto Protocol in 1997 aimed to engage the international community to limit its production of greenhouse gases. Based on these two realities it appears that renewable energies (ENR) may offer the best alternative solution to guarantee a socio-energy, geopolitical and climatic security.

Desalination of seawater and brackish water using solar energy is generating growing interest in some developing countries. The solar desalination technique through the greenhouse effect is based on evaporation–condensation process and dates back to the year 1872 when it was used for the first time on a large scale in the north Chilean desert (1872). Since then, the principle has not changed, although improvements have been obtained in the form of used construction materials and methods of work (Khedim et al. 2004). The

concrete still is a basic reference in greenhouse solar distillation (Tiwari & Lawrence 1991; Ranjan & Kaushik 2013). The main advantages of the greenhouse effect desalination are the water quality produced, and the possibility of integrating different solar thermal energy sources, namely concentrated solar power (CSP). There are four types of CSP technologies; parabolic collectors, fresnel mirrors, solar towers and cylindrical parabolic collectors (CPC), with the earliest in use being the cylindrical parabolic collector. Given that solar distillation has been shown to be technically feasible, simple and profitable to operate (Ranjan & Kaushik 2013), several studies have been carried out in this area to further improve the yield and quality of the distilled water produced (i.e. distilled water quality) as well as to evaluate the importance and utility of the hybrid solar still system.

Bagheri *et al.* (2020) investigated two types of desalination process, an indirect use of solar energy where solar panels and CPC were used for further water heating in the basin, and a direct use of energy generated from solar plates directly in the basin by thermal elements which produced more desalinated water. Tiwari *et al.* (2003) used a continuous water flow over the glass cover coupled with a solar collector to produce more freshwater. In order to overcome this problem, many active solar stills have been developed (Tiwari & Tiwari 2008); the PV-Therm collector (Gaur & Tiwari 2010), reflecting mirror (Fang *et al.* 2018), CPC (Prasad & Tiwari 1996; Ullah & Kang 2019), Flat plate solar collector and TES (El-Sebaï *et al.* 2011) have been used to improve the performance of the traditional solar still. Bellatreche *et al.* (2016) studied the influence of the geometry, seawater mass and TES on the quantity and quality of freshwater. TES improves the freshwater production, due to the continuation of the heat transfer process overnight. Khalifa & Hamood (2009) carried an experimental investigation to validate and enhance the correlation of three parameters of a solar distiller in which the solar still with the higher brine depth has a larger nocturnal production. Voropoulos *et al.* (2003) proposed a model 'input-output' method for the description of the solar still coupled with solar collectors.

Considering the solar energy potential of the Middle East and North Africa (MENA) region and particularly Algeria, this study considered the use of the parabolic trough solar collector technology coupled with thermal energy storage (TES) by sand, in order to improve the

thermal efficiency of the desalination greenhouse process. Sand is an excellent thermal accumulator, it does not degrade and never loses its thermal characteristics during storage and destocking cycles. Sand is a non-polluting material and presents no end-of-life problem, it costs almost nothing. This thermal process is the key to resolving future water problems in the regions with the lowest water content, namely arid and isolated sites. The aim of this study was to assess the heat amount effect delivered by the solar concentrator to the TES system integrated into the solar still. The sensitive storage system was defined by an isolated enclosure equipped with a tubular exchanger trapped in the sand (storage material). This thermal storage will allow estimation of the distillation continuity process. Thus, the distilled water amount produced by the system will be optimized. The hybrid still was compared with conventional concrete still.

MATERIALS AND METHODS

Description of the system

The system is equipped with a solar still consisting of a tank filled with seawater to be treated, stagnant within a tank with a selective absorbent layer. The solar still operates as a hybrid system comprising: the CPC for energy storage and a photovoltaic panel for power to run the circulators. The solar still has a basin area of 1 m² and the reservoir is topped with side walls of an optimized height and covered with a glass inclined at an angle of 20° to fine tune solar radiation transmission and allow an easy flow of water droplets. Figure 1 shows the schematic diagram of the system. The water volume was adjusted to occupy a selected thickness (Bellatreche *et al.* 2016). The mass of seawater is heated by the greenhouse effect in parallel with a heat exchanger connected to a CPC collector containing a heat transfer fluid to concentrate and accelerate the heating process. The heat exchanger is integrated into a sand storage bed to extend the distillation process in the absence of the sunlight.

The choice of sand as the storage material is based on the published study by Taamneh & Al-Shyyab (2016). They experimentally investigated the effect of natural Jordanian

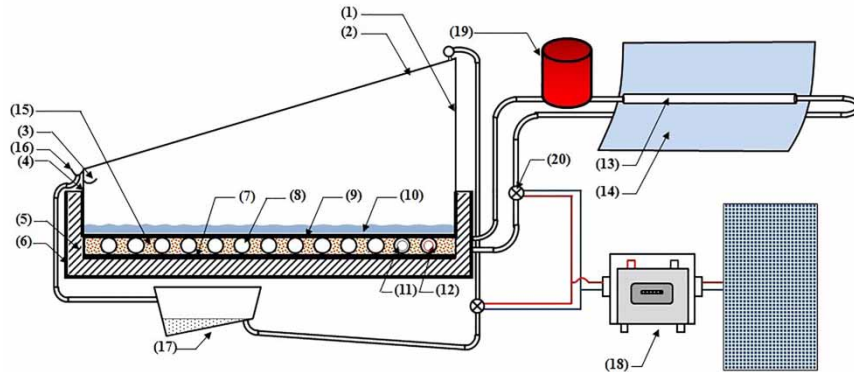


Figure 1 | Solar desalination apparatus with thermal energy storage (TES). Solar still: (1) Rear side wall, (2) Glass, (3) Drain for collecting distilled water, (4) Front side wall, (5) Insulation, (6) Galvanized sheet, (7) Wooden plate, (8) Heat exchanger, (9) Copper plate, (10) Seawater layer, (11) Exchanger outlet, (12) Exchanger inlet, (16) Drain collecting channel cooling water, (13) Absorber tube, (14) Parabolic trough solar collector, (15) Thermal energy storage materials (sand), (17) Cooling and cleaning system, (18) Photovoltaic kit, (19) Fluid storage tank, (20) Circulator.

zeolite as a TES material on the thermal efficiency of a pyramid-shaped solar still. The results showed that the productivity of the solar still can be considerably improved through adding zeolite beneath the water basin. They found that the daily freshwater productivity of the solar still with zeolite increased by about 43%. The obtained experimental results were confirmed with CFD simulation results. It was demonstrated that the CFD results are in good agreement with the experimental results by Taamneh (2016). The storage material type choice (quartz sand) is made based on these thermal characteristics and its availability. The quartz sand thermal aptitude is mainly determined by its SiO_2 content, the higher the content the more the sand behaves favorably against thermal loads. In general, the reference values for the SiO_2 content are between 94 and 99% (Foundry Lexicon 2003). The selected sand rich in quartz has an average content of 98%, found in abundance in the southern regions of Algeria (Grand Sahara). For example, the sand chemical composition of the Bechar–Taghit region is defined by 98.7% of SiO_2 and the remainder include CaCO_3 , Fe_2O_3 , MgO , Al_2O_3 , TiO_2 (Anas Boussaa et al. 2018).

Energy balance computation of hybrid solar still

The thermal model elaborated by (Gaur & Tiwari 2010) was used to determine the heat and mass transfer for the theoretical study of the hybrid solar still with CPC and TES (Figure 2).

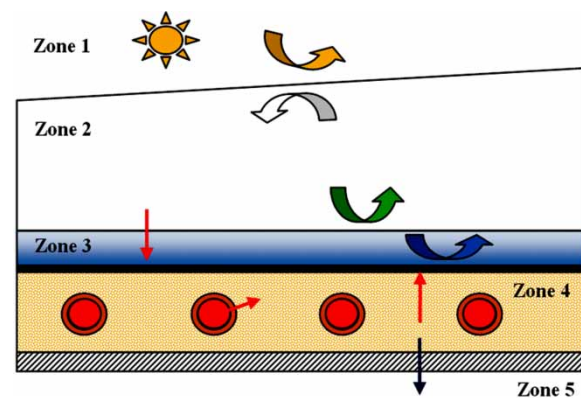


Figure 2 | Thermal balance of solar still with thermal energy storage (TES).

The integral equations of Gaur & Tiwari (2010) were used for the first and second zone. However, the equations of the 3rd, 4th and 5th zones are modified according to the TES integration, with the sand through the heat transfer fluid which flows in the exchanger. The model of Gaur & Tiwari (2010) does not have a storage zone, and the energy given by the plant solar collectors directly heats the seawater (convective transfer). This configuration is totally different compared to the present work (energy supplied to the water basin is conductive in nature).

The thermal balance of each zone is described by the following equations:

Energy balance for outer surface of glass cover (zone 1)

$$\frac{K_g}{e_g} \cdot (T_{gi} - T_{go}) = h_{1g} \cdot (T_{go} - T_a) \quad (1)$$

h_{1g} is the total external heat transfer coefficient and is given as $h_{1g} = 5.7 + 3.8 V_{wind}$

Energy balance for inner surface of glass cover (zone 2)

$$\alpha'_g \cdot I(t) \cdot A_g + h_{zw} \cdot (T_w - T_{gi}) \cdot A_D = \frac{K_g}{e_g} \cdot (T_{gi} - T_{go}) \quad (2)$$

Energy balance for water mass (zone 3)

$$\begin{aligned} \alpha'_w \cdot I(t) \cdot A_D + h_{Dw} \cdot (T_D - T_w) \cdot A_D \\ = M_w \cdot C_w \cdot \left(\frac{dT_w}{dt} \right) + h_w \cdot (T_w - T_{gi}) \cdot A_D \end{aligned} \quad (3)$$

Energy balance for basin liner (zone 4)

$$Q_{CPC} + \alpha'_D \cdot I(t) \cdot A_D = h_{Dw} \cdot (T_D - T_w) \cdot A_D + h_{Ds} \cdot (T_D - T_s) \cdot A_D \quad (4)$$

Energy balance for trough collector (zone 5)

$$Q_{CPC} = h_{Dw} \cdot (T_D - T_s) \cdot A_D + h_{Da} \cdot (T_D - T_a) \cdot A_D \quad (5)$$

The solution of Equation (3) allows the water temperature T_w (t) to be a function of the CPC flux in function of the time t:

$$\begin{aligned} T_w(t) = \frac{123 I(t)}{100 h_w} + T_{gi} + \frac{2 Q_{CPC}}{h_w} \\ + e^{-\frac{9 h_w}{10 M_w} \left(T_{w0} - \frac{123 I(t)}{100 h_w} - T_{gi} - \frac{2 Q_{CPC}}{h_w} \right)} \end{aligned} \quad (6)$$

where T_{w0} is the initial temperature of the basin at $t = 0$.

The radiation values and the wind velocity were recorded in the weather station of UDES Bou-Ismaïl. The heat transfer fluid used in this analysis is ethylene glycol with an evaporation temperature of $T_{ev} = 471$ K. The physical and chemical characteristics of materials utilized are given in Table 1.

The evaporation mass M_{ew} is calculated directly from Equation (7). The freshwater mass harvested is defined in Equation (15).

Table 1 | Physico-chemical characteristics of used materials (Engineering ToolBox 2003)

Type	Cp (J/kg.K)	Thermal conductivity (W/m.K)	fraction of solar flux absorbed α'
Quartz sand (Anas Boussaa et al. 2018)	835	0.8	-
Copper, tarnished, black	385	390	0.89
Seawater	4,000	2.3	0.34
Ethylene glycol	2,400	0.26	-

The rate of mass evaporation and evaporative heat loss can be obtained as (Gaur & Tiwari 2010):

$$M_{ew} = \frac{\dot{Q}_{ew}}{L} \quad \text{and} \quad \dot{Q}_{ew} = h_{ew}(T_w - T_{gi}) \quad (7)$$

The evaporative heat transfer coefficient (h_{ew}) is determined as:

$$h_{ew} = 0.01623 \times h_{cw}(P_w - P_{gi}) \times (T_w - T_{gi})^{-1} \quad (8)$$

For a solar still, the convective heat transfer coefficients (h_{cw}) is given as (Dunkle 1961):

$$h_{cw} = 0.884 (\Delta T)^{1/3} \quad (9)$$

where

$$\Delta T = [T_w - T_{gi} + (P_w - P_{gi})(T_w + 273) \times (268.9 \times 10^3 - P_w)^{-1}]^{1/3} \quad (10)$$

and

$$P_w = \exp\left(25.317 - \frac{5144}{T_w + 273}\right) \quad (11)$$

$$P_{gi} = \exp\left(25.317 - \frac{5144}{T_{gi} + 273}\right) \quad (12)$$

The radiative heat transfer coefficient is given as:

$$\begin{aligned} h_{rw} = \epsilon \times 5.67 \times 10^{-8} \\ \times \{[(T_w + 273)^4 - (T_{gi} + 273)^4] \times (T_w - T_{gi})^{-1}\} \end{aligned} \quad (13)$$

After calculating the values of convective, radiative and evaporative heat transfer coefficients, the total heat transfer coefficient is computed as:

$$h_w = h_{cw} + h_{ew} + h_{rw} \quad (14)$$

Finally, the distillate output is evaluated by using (Gaur & Tiwari 2010):

$$\dot{Q}_w = M_{ew} \times A_g \times t \quad (15)$$

Computational fluid dynamic model: CPC and TES system

The CFD Ansys Fluent code was used for the present simulation. It allowed modeling of fluid mechanics mass and heat transfer problems, based on the finite volume method. Two equations are used in this work concerning Flow and Energy in unsteady laminar mode. The relationship between velocity and pressure corrections (pressure-velocity coupling) to enforce mass conservation was effectuated by the 'SIMPLE' algorithm. The second order was employed for the spatial pressure discretization. The 3D thermal analysis consists of two parts:

- (1) The simulation of CPC absorber.
- (2) The heat transfer between the sand storage bed and copper tubular exchanger (Figure 3).

The CPC absorber is a copper tube with $L_{abs} = 1.4$ m and $R_{abs} = 0.04$ m, with an 870,000 structured mesh, tight at the walls. The heat transfer fluid inlet velocity (ethylene glycol) into the absorber is set at $Vf_{abs} = 0.5$ m/s.

The solar irradiative flux received by the absorber consists of two parts, direct solar radiation flux, and flux

concentrated by the parabolic trough collector with a geometric concentration factor $C_f = 21.9$, defined as a ratio of the reflector opening area A_{ref} to that of the absorber A_{abs} .

It is considered that the solar radiation is constant during the same hour and that the heat transfer fluid is incompressible (Figure 3(a)). Depending on the computing capacity, and geometry symmetry consideration, a numerical computational volume specific to the storage system was adopted, in order to determine the sand temperature. The considered volume dimensions are $(16 \times 16 \times 32) \times 10^{-3}$ m, i.e. 8.2×10^{-6} m³, with a copper exchanger tube of a radius $R_{exch} = 0.007$ m and a thickness of $e_{exch} = 0.001$ m. The exchanger with a length of 7.2 m is embedded in a sandbox which is in contact with the solar still copper base. The heat transfer fluid circulation velocity in the exchanger is $Vf_{exch} = 2.5$ m/s. The exchanger inlet temperature is the average CPC absorber outlet temperature, which is considered constant along the exchanger, during a time interval of one hour (depending on the solar radiation during the day) (Figure 3(b)).

Theoretical model validation: comparison with the experimental results

The developed numerical model is validated against the concrete solar still experimental results in square geometry carried out at the Bou-Ismaïl (Algeria) site in May 2014 (Bellatreche et al. 2016). Table 2 presents the comparison of the daily distillation between the concrete still experimental and the theoretical results for the developed model as a function of the seawater volume. The model absolute average precision is estimated at 8.7%. However, the minimum default error is -7%. The accepted error for the different models proposed in the specialized literature is about

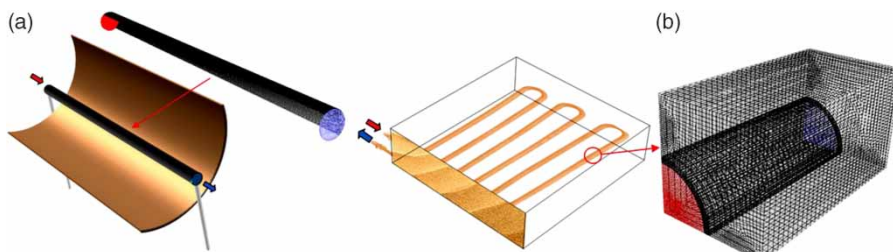


Figure 3 | Computational domain, geometry and mesh. (a) Cylindrical parabolic collector (absorber), (b) Sand storage bed and heat exchanger.

Table 2 | Comparison of daily distillate yield between theoretical and experimental results

Seawater volume V_{w0} (l)	25	35	45
Theoretical production (l) [Equation (15)]	4.05	3.03	1.85
Experimental production (l) (Bellatreche <i>et al.</i> 2016)	3.6 ± 0.1	3.5 ± 0.1	2.1 ± 0.1
Relative error (%)	+9	-10	-7

5–10% (Tiwari *et al.* 2003; Shalaby *et al.* 2016; Mahmoud *et al.* 2019). The present model is included in the tolerated error interval.

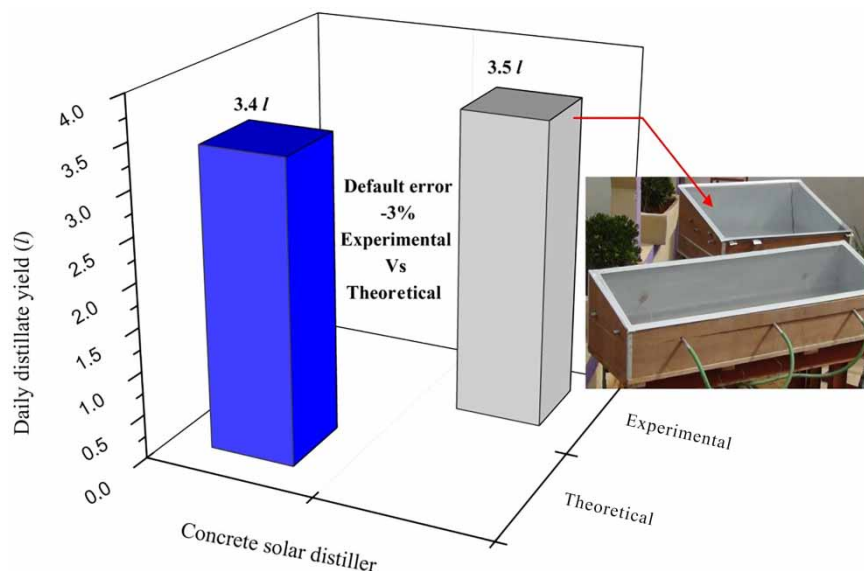
The average error 8.7% is explained by the following assumptions which neglect in the theoretical model:

- The pressure losses in the pipes.
- The salt deposits at the still tank bottom and the variation in the seawater density to be distilled.
- Heat transfer at the solar still side walls.
- The distillate losses at the maximum production hours by the gravity effect.
- The stratification in water mass and the added seawater temperature.
- Wind velocity effect (The experimental wind velocity values are not the same for the seawater volumes studied).

The relative error of daily distillate yield between experimental and theoretical result ($M_{w0} = 35$ kg) is -3% (default error) after the wind velocity effect introduction $V_{wind} = 4.16$ m/s (Equation (1)). The error has decreased from -10% to -3% considering the wind velocity (Equation (1)) (Figure 4). The wind favors the solar still glass cooling by forced convection, this cooling accelerates the condensation process at the interior glass level by increasing the temperature gradient between the two medium (fluid-wall interaction).

The increase in the seawater volume to be distilled implies a decrease in the freshwater production (Gaur & Tiwari 2010), due to the seawater warming process slowness. However, for low volumes the acceleration of the evaporation process induces an increase in salt concentration and deposits at the distiller basin base, reducing the solar radiation absorption by the black coating.

According to the specific experimental results to the distiller geometry and the climatic conditions for a several days, it was found that the optimum mass to be distilled corresponds to $M_{w0} = 35$ kg (Bellatreche *et al.* 2016). Based on the freshwater yield produced and its variation depending on the initial seawater volume, the concordance criterion between theoretical and experimental results was imposed. The theoretical model behavior is in good agreement with the experimental values for the same weather conditions.

**Figure 4** | Theoretical model validation by the experimental result (Bellatreche *et al.* 2016). ($M_{w0} = 35$ kg and wind velocity influence.)

RESULTS AND DISCUSSION

Hourly absorber CPC and sand temperatures

The CFD simulation is the first step in this study. It allows the quantification of heat flux Q_{cpc} captured by the CPC at the absorber tube level and transferred to the storage material (quartz sand) through the copper exchanger buried in the sandbox (Figure 5).

The temperatures at the outlet absorber tube T_{cpc} and of the storage material (quartz sand) T_{sand} are determined numerically by CFD simulation. These temperatures vary according to the daily solar radiation. The maximum day solar radiation is recorded at 12 p.m., $I = 845 \text{ W/m}^2$, with a relatively constant ambient temperature $T_{a/avg} = 291 \text{ K}$. The temperatures T_{cpc} and T_{sand} continue to increase until reaching their maximum values at 7 p.m. $T_{cpc/max} = 311 \text{ K}$ and $T_{sand/max} = 303.8 \text{ K}$, just before sunset, despite the decrease in solar radiation after 12 p.m. However, a difference of -19% between the two temperatures at the same hour was observed (Figure 5).

The ethylene glycol velocity ($T_{f0} = 294 \text{ K}$) at the heat exchanger $Vf_{exch} = 2.5 \text{ m/s}$ and the absorber tube $Vf_{abs} = 0.5 \text{ m/s}$ relative to the Reynolds numbers $Re_{exch} = 1,966$ and $Re_{abs} = 2,247$ respectively correspond the laminar flow regime (Firdaous et al. 2015). However, at higher temperatures ($T_f = 313 \text{ K}$) and for the same velocity, Reynolds numbers recorded are $Re_{exch} = 3,885$ and $Re_{abs} = 4,440$. These values define a pre-turbulent transition regime

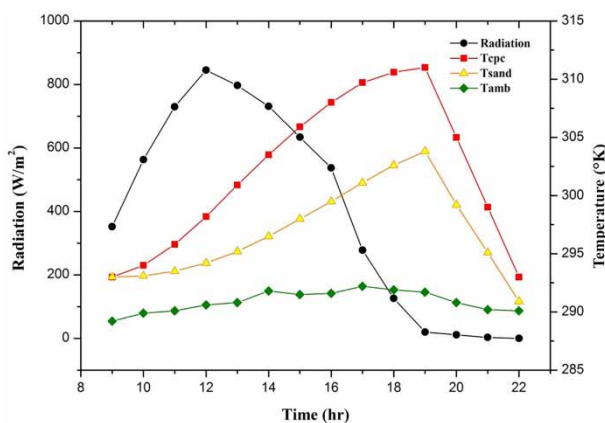


Figure 5 | Hourly variation of absorber CPC and sand temperatures.

(Firdaous et al. 2015), promoting heat exchange and minimizing pressure losses, contrary to the developed turbulence regime. The temperature has a direct influence on the heat transfer fluid viscosity variation, which is clearly observed on the flow regime (+97.6% on the Reynolds number). The flow regime influence on the heat transfer coefficient h is represented in an intrinsic manner via the heat flux Q_{cpc} .

Solar distiller hourly CPC flux

The CFD approach enables the determination of heat transfer fluid temperatures T_{abs} and the exchanger temperatures T_{exch} , from the daily solar radiation concentrated by the collector (Figure 6). These results are used in the hybrid still energy balance to determine the influence of Q_{cpc} on the distilled water production Pr .

The flux yielded by the sand to the solar still reaches its maximum value at 5 p.m. with $\phi_{cpc} = 75 \text{ W/m}^2$. The CPC flux daily evolution as a function of the temperature T_{cpc} is defined by a Gaussian curve. The total daily flow received by the still is $\Sigma\phi_{cpc} = 592 \text{ W/m}^2$ (Figure 6). The storage of the energy produced by the parabolic trough collector and additional flux strongly depends on the system weather and initial conditions.

Solar distiller daily yield

This section deals with the dual influence of the solar distiller basin material (concrete or copper) and the CPC heat flux transferred to the seawater mass, on the daily freshwater production Pr (Equations (7) and (15)) for a single day. Using tarnished copper instead of concrete increases the daily water production from 3.4 l to 5.1 l , it presents $+50\%$ of the production Pr . However, the combination of copper plus CPC thermal flux offers a production gain of 3.1 l ($3.4 \text{ l} - 6.5 \text{ l}$). This improvement correspond a $+91\%$ of the traditional concrete solar still production for the same meteorological conditions (ambient temperature, solar irradiation and wind velocity) (Figure 7).

These results can be explained on the one hand by the copper super thermal conductivity and the black coating with high solar radiation absorption and on the other hand, by the additional flux Q_{cpc} (Equations (4) and (5))

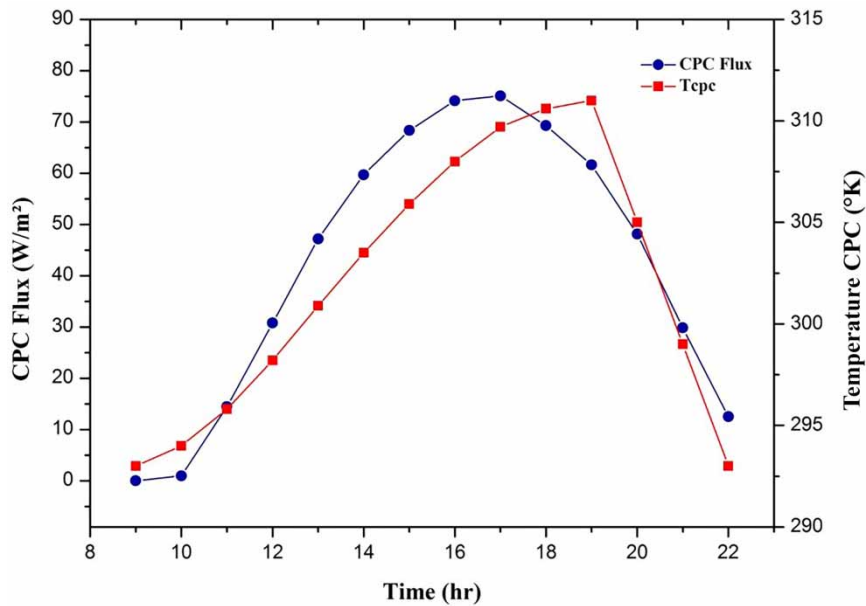


Figure 6 | Hourly flux variation and temperature variation of CPC absorber.

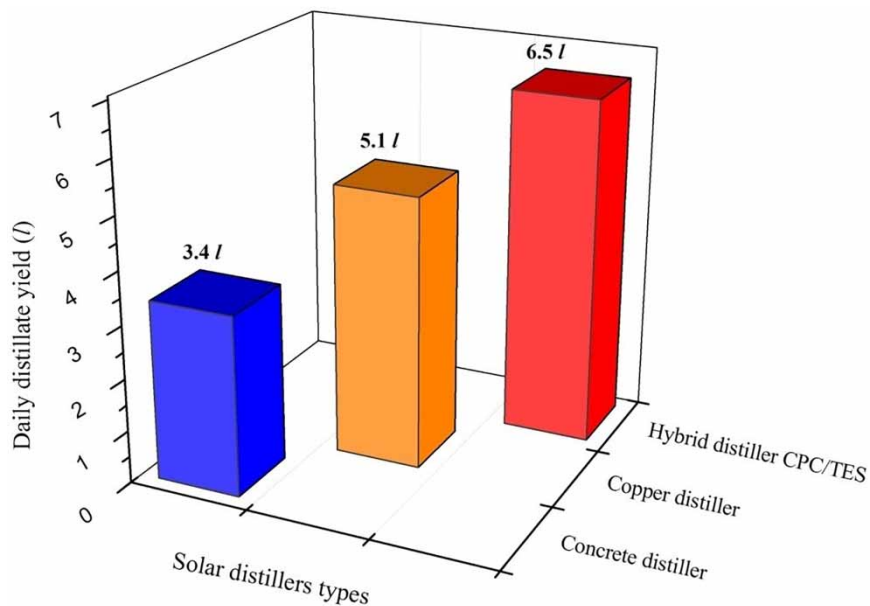


Figure 7 | Theoretical variation of the daily freshwater yield for the solar distiller types.

transmitted via the sandbox to the solar still, accelerating the evaporation process by increasing the seawater temperature T_w (Equation (6)). The influence of extra thermal flux on the daily yield improvement has been illustrated in the specialized literature by several studies (Table 3).

Solar distiller hourly yield

The seawater temperature during the day changes according to the daily solar radiation. It has the same appearance for the three types of solar still (concrete, copper and hybrid).

Table 3 | Improvement freshwater daily production for hybrid solar still

Additional thermal flux system	Freshwater daily production	References
PV-Therm collector (Collector Nbr)	+27% (02) +211 (10)	Gaur & Tiwari (2010)
Mirror reflector + lenses	+ 29%	Fang et al. (2018)
Flat plat solar collector + direct storage	+ 55%	El-Sebaili et al. (2011)
Flat plat solar collector + Indirect storage	+ 23%	Bellatreche et al. (2016)
CPC direct system	+ 65%	Prasad & Tiwari (1996)
CPC	+ 35%	Ullah & Kang (2019)
CPC + TES indirect system	+ 91%	Present study

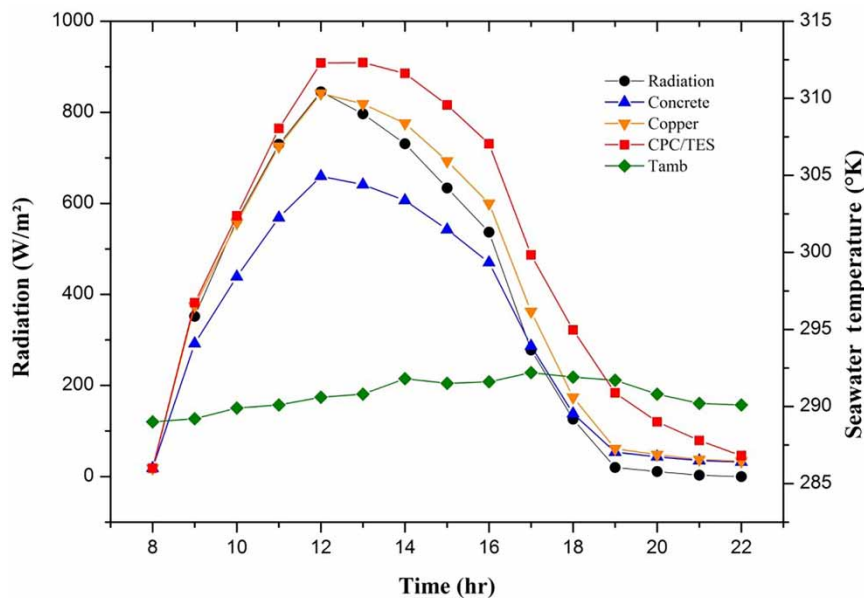
The maximum temperature values T_w are recorded between 12 p.m. and 4 p.m. (Figure 8), with $T_{w,cpc/max} = 312.3$ K. Its average temperature T_w during the same period is $T_{w,cpc/avg} = 310.6$ K, which represents an increase of +26.6% compared to the concrete solar still (Table 4). Effectively, the variation in seawater temperature is closely linked

Table 4 | Average seawater temperature and production variations with solar distiller type (12 p.m. to 4 p.m.)

Solar distiller type	$T_{w/avg}$ (K)	$Pr_{w/max}$ (l)	$Pr_{w/avg}$ (l/hr)	ΣPr_w (l)
Concrete	302.7	0.53	0.39	1.56
Copper	307.5 +16.2%	0.90	0.70 +79.5%	2.80
Hybrid CPC/ TES	310.6 +26.6%	1.14	0.98 +151.3%	3.92

to solar radiation during the day. Solar radiation is responsible for the greenhouse effect, the principal mechanism in the evaporative-condensation distillation process. This thermal source is both direct or principal (radiation received directly at the distiller level) and indirect or secondary (radiation absorbed by the heat transfer fluid at the CPC level). Part of this secondary source allows the seawater temperature of the hybrid still to be higher by +26% compared to the conventional concrete still. The other part is stored at sand level. A more detailed study will allow quantification of storage and destocking over several days of operation.

The hourly yield becomes maximal at 1 p.m. due to high water temperature which increases the value of evaporative heat transfer coefficient. The maximum daily yield value is

**Figure 8** | Hourly variation of solar radiation and seawater temperature for different solar distiller type.

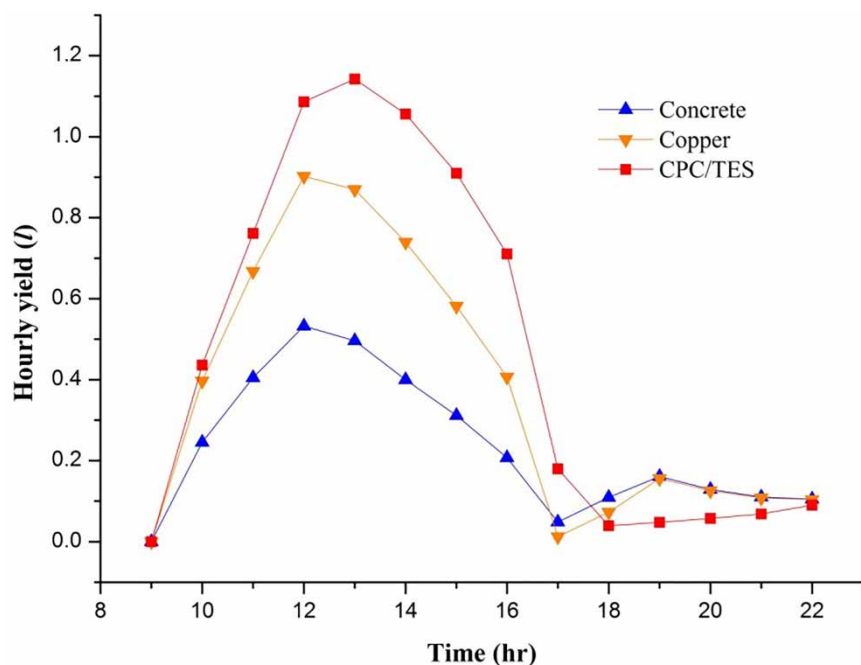


Figure 9 | Hourly yield variation of concrete, copper and hybrid solar distiller.

related to the hybrid solar distiller $T_{w-cpc/max} = 1.14 l$. However, the average hourly yield value recorded between 12 p.m. and 4 p.m. is $0.98 l/hr$ ($\Sigma Pr_w = 3.92 l$ which represents 60%). This value represents a growth of +151.3% compared to the quantity produced by the concrete solar still (Table 4). Between 9 a.m. and 12 p.m., the amount hourly yield value is $\Sigma Pr_w = 2.28 l$ (35%). Between 4 p.m. and 8 p.m., the amount hourly yield value is $\Sigma Pr_w = 0.32 l$ (5%) (Figure 9).

In the period between 12 p.m. and 4 p.m., the radiative energy flux absorbed by the copper is greater than that absorbed by the concrete, due to the material thermal effusivity ($611 J/K \cdot m^2 \cdot s^{1/2}$ for copper and $23.6 J/K \cdot m^2 \cdot s^{1/2}$ for concrete), with a ratio of 23 times. The copper low thermal inertia is compensated by the TES introduction.

CONCLUSION

Following the modifications to a traditional solar greenhouse concrete still defined by additional thermal CPC flux, TES (quartz sand) and distiller basin material

(tarnished copper) for a seawater mass of 35 kg, the main findings and perspective are:

- The additional CPC system and TES have a positive effect on the solar distiller performance +91%. However the TES influence has not a significant impact during the experiment first phases, for this a more detailed study will allow quantification of storage and destocking over the alternation day/night and for several operation days.
- It is important to properly size the storage tank (heat transfer fluid) in order to ensure the heat source alternation.
- The choice of the additional thermal flux process is strongly dependent on the basin solar still material to improve the freshwater daily yield production.
- The hybrid solar still daily efficiency is proportional to the solar radiation. It is more gainful on the socio-economic plan for desert regions (Sahara).

DATA AVAILABILITY STATEMENT

All relevant data are included in the paper or its Supplementary Information.

REFERENCES

- Anas Boussaa, S., Kheloufi, A. & Boutarek Zaourar, N. 2018 Sand dune characterization for preparing metallurgical grade silicon. *Open Chemistry* **16**, 1227–1232.
- Bagheri, A., Esfandiari, N., Honarvar, B. & Azdarpour, A. 2020 An experimental study on the effects of direct and indirect use of solar energy on solar seawater desalination. *Water Supply* **20** (1), 259–268.
- Bellatreche, R., Belhout, D., Ouali, M., Zioui, D., Tigrine, Z., Aburideh, H. & Hout, S. 2016 Thermo-energy transfer optimization of a solar distiller with energy storage under Bou-Ismaïl climatic conditions. In: *Renewable Energy in the Service of Mankind. II*, Chap. 62, 1st edn (A. Sayigh, ed.). Springer International Publishing, Switzerland, pp. 691–701. <https://doi.org/10.1007/978-3-319-18215-5>.
- Dunkle, R. V. 1961 Solar water distillation, the roof type still and a multiple effect diffusion still. In *International Developments in Heat Transfer, ASME. Proceedings of International Heat Transfer Conference, Part V*. University of Colorado, p. 895.
- Eau 2019 Available from: <https://www.banquemonde.org/fr/topic/water/overview>.
- El-Sebaï, A. A., Aboul-Enein, S., Ramadan, M. R. I. & Khallaf, A. M. 2011 Thermal performance of an active single basin solar still (ASBS) coupled to shallow solar pond (SSP). *Desalination* **280**, 183–190.
- Engineering ToolBox 2003 *Ethylene Glycol Heat-Transfer Fluid*. Available from: https://www.engineeringtoolbox.com/ethylene-glycol-d_146.html (accessed 20 June 2020)
- Fang, S., Tu, W., Zhu, L. & Sun, Z. 2018 Sunlight concentration effect analysis of lenses on single-slope solar still. *Water Science & Technology: Water Supply* **18** (6), 1888–1896.
- Firdaus, L., Dimitrov, K. & Vauchel, P. 2015 *Introduction au GIA, Notions de base de mécanique des fluides, Université de Lille-Sciences et Technologies*. Available from: https://tech-alim.univ-lille.fr/intro_gia/co/ch03_01.html (accessed 02 July 2020).
- Foundry Lexicon 2003 Quartz sand. Available from: <https://www.giessereilexikon.com/en/foundry-lexicon/Encyclopedia/show/quartz-sand-4514/?cHash=de60089e1bbd9c508829aae856425a68> (accessed 22 June 2020).
- Gaur, M. K. & Tiwari, G. N. 2010 Optimization of number of collectors for integrated PV/T hybrid active solar still. *Applied Energy* **87**, 1763–1772.
- Khalifa, A. J. N. & Hamood, A. M. 2009 Experimental validation and enhancement of some solar still performance correlations. *Desalination & Water Treatment* **4**, 311–315.
- Khedim, A., Klemens, S., Christian, F. & Christoph, M. 2004 Production décentralisée de l'eau potable à l'énergie solaire. *Desalination* **168**, 13–20.
- Mahmoud, A., Fath, H., Ookwara, S. & Ahmed, M. 2019 Influence of partial solar energy storage and solar concentration ratio on the productivity of integrated solar still/humidification-dehumidification desalination systems. *Desalination* **467**, 29–42.
- Prasad, B. & Tiwari, G. N. 1996 Effect of glass cover inclination and parametric studies of concentrator-assisted solar distillation system. *International Journal of Energy Research* **20** (6), 495–505.
- Ranjan, K. R. & Kaushik, S. C. 2013 Energy, exergy and thermo-economic analysis of solar distillation systems: a review. *Renewable and Sustainable Energy Reviews* **27**, 709–723.
- Shalaby, S. M., El-Bialy, E. & El-Sebaï, A. A. 2016 An experimental investigation of a v-corrugated absorber single-basin solar still using PCM. *Desalination* **398**, 247–255.
- Taamneh, Y. 2016 Influence of Jordanian zeolite on the performance of a solar still: experiments and CFD simulation studies. *Water Science & Technology: Water Supply* **16**, 1700–1709.
- Taamneh, Y. & Al-Shyyab, A. 2016 Improvement of the performance of a solar still by utilizing the sorption thermal storage of natural zeolite. *Desalination & Water Treatment* **57**, 27450–27457.
- The Global Risks Report 2016 11th edn, Published by the World Economic Forum Within the Framework of the Global Competitiveness and Risks Team, REF:080116. Available from: <http://wef.ch/risks>.
- Tiwari, G. N. & Lawrence, S. A. 1991 Experimental evaluation of solar distiller units with FRP lining under PNG climatic conditions. *International Journal of Solar Energy* **9**, 241–248.
- Tiwari, G. N. & Tiwari, A. K. 2008 *Solar Distillation Practice for Water Desalination Systems*. Anamaya Publisher, New Delhi.
- Tiwari, G. N., Shukla, S. K. & Singh, I. P. 2003 Computer modeling of passive/active solar stills by using inner glass temperature. *Desalination* **154** (2), 171–185.
- Ullah, F. & Kang, M. 2019 Performance evaluation of parabolic trough solar collector with solar tracking tilt sensor for water distillation. *Energy & Environment* **30**, 1219–1235.
- UNICEF 2017 Progrès en matière d'approvisionnement en eau potable, d'assainissement et d'hygiène. [Progress on drinking water, sanitation and hygiene: 2017], Organisation mondiale de la Santé et le Fonds des Nations Unies pour l'enfance (UNICEF). Available from: <http://apps.who.int/iris>. ISBN 978-92-4-251289-2.
- Voropoulos, K., Mathioulakis, E. & Belessiotis, V. 2003 Solar stills coupled with solar collectors and storage tank analytical simulation and experimental validation of energy behavior. *Solar Energy* **75**, 199–205.

First received 27 January 2021; accepted in revised form 26 April 2021. Available online 6 May 2021